International Journal of Microwave and Wireless Technologies

cambridge.org/mrf

A printed multiband MIMO antenna with decoupling element

Ziyu Xu, Qisheng Zhang and Linyan Guo

School of Geophysics and Information Technology, China University of Geosciences, Beijing, China

Research Paper

Cite this article: Xu Z, Zhang Q, Guo L (2019). A printed multiband MIMO antenna with decoupling element. *International Journal of Microwave and Wireless Technologies* **11**, 413–419. https://doi.org/10.1017/S1759078719000096

Received: 9 April 2018
Revised: 15 January 2019
Accepted: 20 January 2019
First published online: 1 March 2019

Key words:
Multiple-input multiple-output (MIMO) antenna; multiband; decoupling; printed monopole; 5G

Author for correspondence:
Linyan Guo, E-mail: guoly@cugb.edu.cn

Abstract

A printed multiband Multi-Input Multiple-Output (MIMO) antenna is proposed in this paper. This MIMO antenna system comprises two symmetric printed monopole antennas. Each antenna element consists of multiple bend lines, producing four resonant modes and covering the GSM900, PCS, LTE2300, and 5G bands. Simulated and measured results prove that the proposed MIMO antenna can be applied to traditional 2G, 3G, 4G, and present 5G mobile communication. By etching four inverted *L*-shaped grooves on its ground plate, mutual coupling between the adjacent antenna elements has been suppressed. This makes the $|S_{21}|$ at all four resonant modes is lower than −40 dB. In addition, its low coupling mechanism has been analyzed by surface current distribution. The designed multiband MIMO antenna provides an idea of reference to realize low mutual coupling between antenna elements, which is also realizable in infrared or optical regimes with appropriate designs.

Introduction

Multiple-Input Multiple-Output (MIMO) technology is considered as a core technology for next generation mobile communication. In order to increase network throughput, communication capacity, and coverage without requiring additional bandwidth, MIMO technology can be utilized [1]. Nevertheless, when MIMO antenna is installed in the limited place, the distance between antenna elements is close, it may cause a strong mutual coupling. As a result, the size of the MIMO antenna is relatively large, and the throughput of the communication is decreased [2, 3].

In recent years, several antenna designs have been proposed in MIMO terminals. However, there is a strong coupling problem caused by the close distance of the MIMO antenna, which may greatly affect the performance of the antenna. For example, antenna gain and radiation efficiency may be reduced. In order to overcome the above problems, several methods and researches are devoted in this field. For instance, in order to reduce the mutual coupling for a planar MIMIO antenna, [4, 5] provide a defected ground structures with two resonances. Rahmat-Samii and Mosallaei and Li and Feresidis propose electromagnetic band-gap structures in [6, 7]. Literatures [8, 9] provide meandering branch-shape to implement the decoupling. In [10], the authors analyze the influence of the three structures of split-ring resonator, non-bianisotropic split-ring resonator, and spiral resonator on the decoupling. In addition, a capacitive coupling between the π-line and the two curved stubs is adopted to form the decoupling network [11]. Furthermore, a novel diamond-shaped patterned ground resonator is used to achieve the decoupling [12]. Two bent slits are etched on the ground plane to reduce coupling in [13]. A *T*-shaped strip on the ground is employed to further improve the isolation for low frequency [14]. Moreover, in [15], it reports a neutralization line technique to achieve decoupling. Then authors of [16] presented the use of 3D anisotropic metamaterials to implement the decoupling structures. The above literatures basically cover the 2G, 3G, and 4G band, but the latest proposed 5G has not yet been covered. Now 5G is the most popular research period. It has the advantages of high performance, low latency, and high capacity characteristics. It is the trend of development in the field of mobile communications.

In this paper, we present a compact dual-element printed MIMO antenna that is developed to support the GSM900, PCS, LTE2300, and 5G bands. The proposed antenna is implemented using two symmetrical printed monopole arrays. Compared with a single antenna, two antennas increase the gain of the antenna. This paper introduces a new decoupling structure, consisting of four inverted-*L* branches etched on its ground plane. It can reduce the mutual coupling between two antenna elements. Section 2 details the MIMO antenna configuration. In Section 3, we will discuss the simulated and measured results. At the same time, the proposed decoupling element is described and analyzed in detail.

Antenna design

Figure 1 shows the structure of the proposed multiband MIMO antenna. This MIMO antenna consists of feed line, two bent radiating antennas, and decoupling element. In this paper, a

CAMBRIDGE UNIVERSITY PRESS

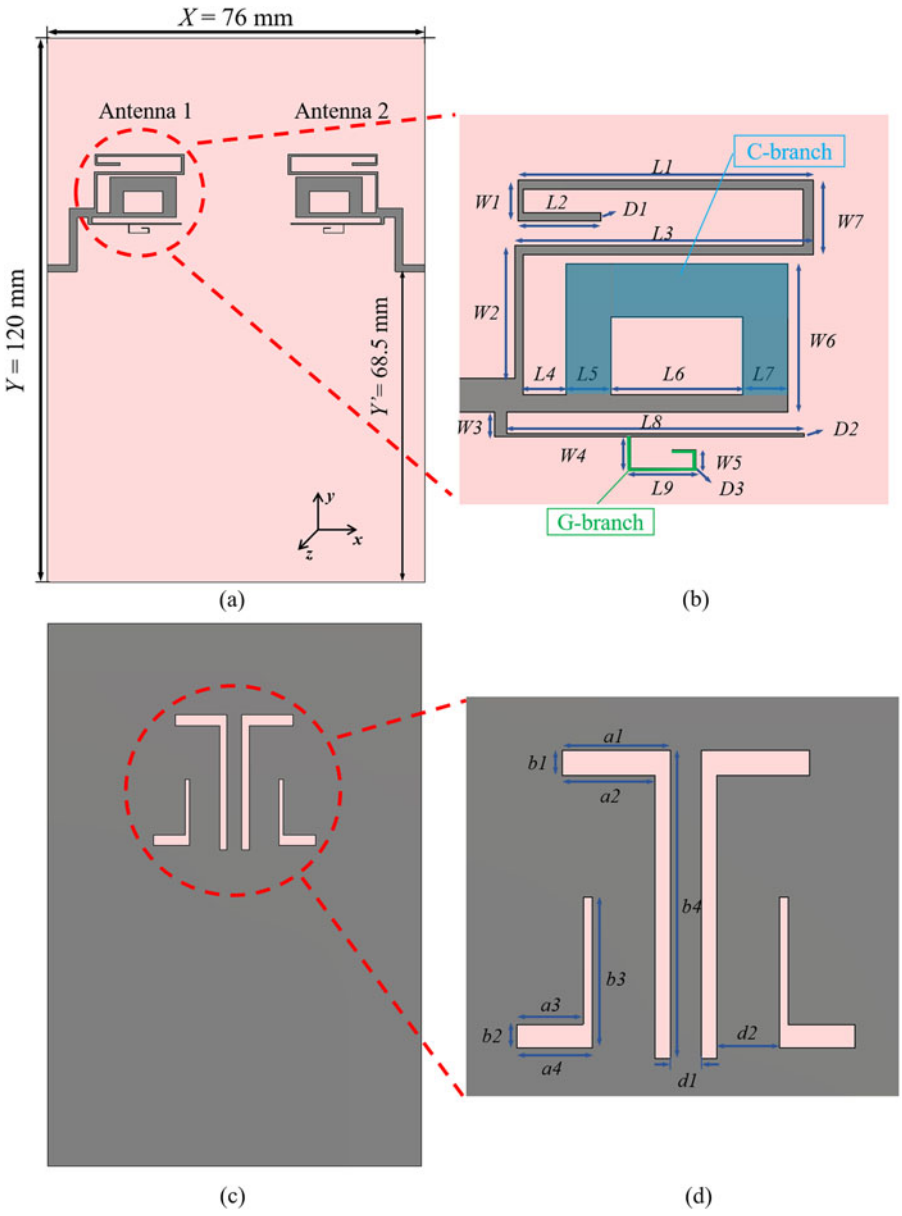

Fig. 1. (a) Top view of the proposed antenna, (b) an enlarged view of the radiation elements, (c) bottom view of the proposed antenna, (d) an enlarged view of the decoupling elements.

1 mm-thick FR-4 (lossy) ($\varepsilon_r = 4.3$, $\tan\delta = 0.025$) is used as the substrate. The size of the substrate and ground plane is $X \times Y = 120 \times 76$ mm^2. The metal we used here is copper whose conductivity is $\sigma = 5.8 \times 10^7 S/m$ and thickness is 0.05 mm.

Figure 1(a) shows the top view of the proposed MIMO antenna. Two radiating patches are symmetrically arrayed on left and right sides of the substrate. The antennas 1 and 2 have the same structure, thus they can operate at the same frequency. In order to maximize transmission power, impedance matching is required. Therefore, it is necessary to adjust the impedance of the antenna feed to 50Ω to match the standard SMA connector. In this model, the resonant frequency and the resonance strength of the MIMO antenna are mainly dependent on the parameters of the individual bent lines. Different branches make them have different electrical lengths. Therefore, the parameters of each bent line are optimized by simulation so that the return loss at the desired resonant frequency becomes less than −10 dB. The specific sizes of the proposed antenna are shown in Fig. 1(b) and listed in Table 1.

In order to cover the 5G band recently proposed by the Ministry of Industry and Information Technology of China, the branch L_8 and its next G-branch (green lines in the picture) of the antenna are added. Hence, each printed monopole antenna element can generate four resonant modes at 0.93, 1.86, 2.32, and 4.87 GHz simultaneously. Besides, the size of L_1 and W_1 mainly affect the resonant frequency at 0.93 GHz. Moreover, the frequency at 1.86 GHz strongly depends on branch L' ($L' = L_4 + L_5 + L_6 + L_7$) and C-branch (blue parts in the picture) where W_6 is located. The frequency adjustment at 2.32 GHz mainly counts on branches L_2 and L_3.

Since these two antennas locate so close to each other, there is a strong coupling between them. The distance between the two antenna elements is $3\lambda_{GSM900}$, $1.5\lambda_{PCS}$, $1.2\lambda_{LTE2300}$, and $0.18\lambda_{5G}$ of the four resonance point medium, respectively. In order to reduce the mutual coupling between them, we introduce an original decoupling element. This decoupling element, consisting of two symmetrical inverted-L branches etched on the ground plane, which is on the bottom layer of the substrate. This structure

https://doi.org/10.1017/S1759078719000096 Published online by Cambridge University Press

Table 1. Specific parameters of the proposed MIMO antenna (unit: mm)

L_1	L_2	L_3	L_4	L_5	L_6	L_7	L_8
17.85	4.7	18.45	2.6	2.8	8	2.7	18
L_9	W_1	W_2	W_3	W_4	W_5	W_6	W_7
4	2.45	10	1.5	2	1	8.9	4.45
D_1	D_2	D_3	a_1	a_2	a_3	a_4	b_1
0.5	0.2	0.1	10.5	9	6.5	7.4	2.5
b_2	b_3	b_4	d_1	d_2			
2.3	14.65	30	3	6.1			

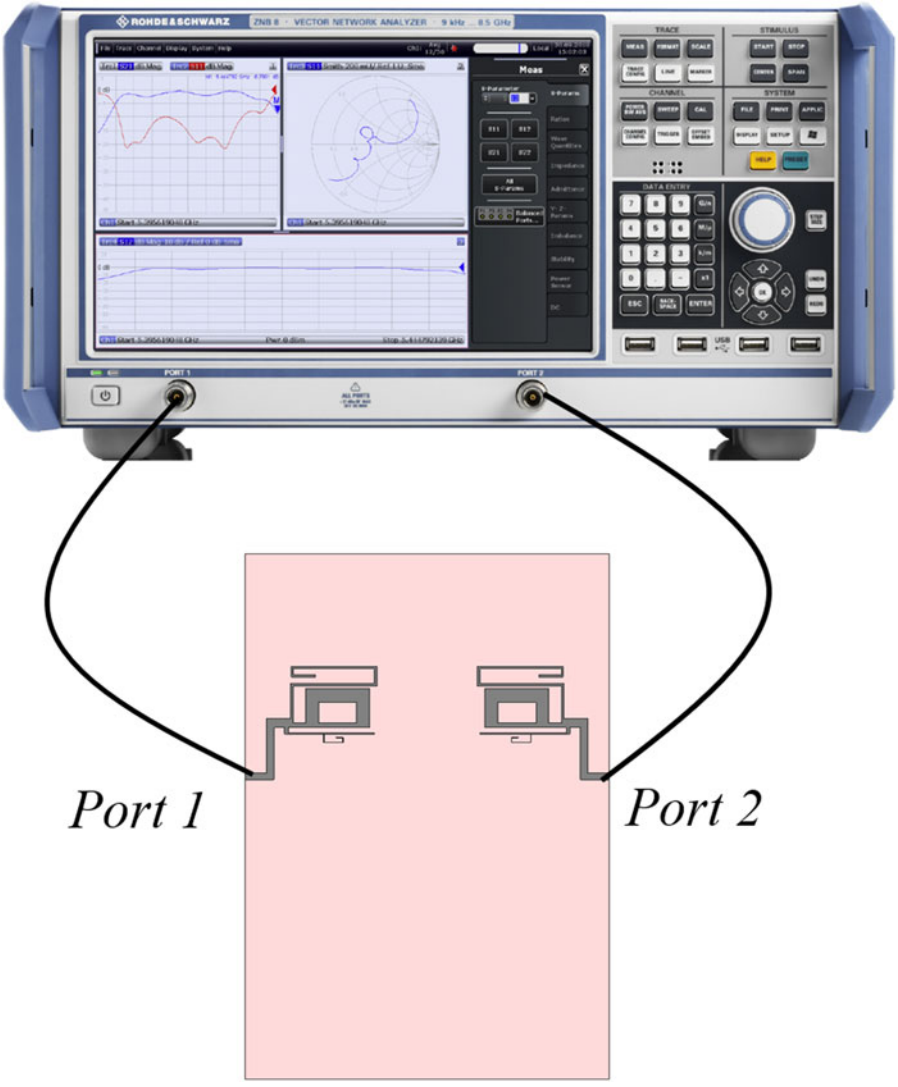

Fig. 2. Experimental test schematic (using Rohde & Schwarz ZNB8).

is shown in Fig. 1(c), and the specific size is shown in Fig. 1(d). The distance between the two symmetrical inverted-L structures is 3 and 18.2 mm, respectively. The initial size of the decoupling structure is determined according to the formula $\lambda_g = c/(f \cdot \sqrt{\varepsilon_r})$. Decoupling can be achieved by adjusting the width and length of the inverted L-shaped structure. Through simulation, the relevant sizes are continuously adjusted and the final determination of the specific parameters of each part is also listed in Table 1. The parameter b_4 of the larger inverted-L structure mainly affects the coupling at 2.32 GHz. While decoupling at 4.87 GHz mainly depends on modifying the size of b_3 and a_4 of the smaller inverted-L branch. Through fine tuning, high isolation has been achieved for the

https://doi.org/10.1017/S1759078719000096 Published online by Cambridge University Press

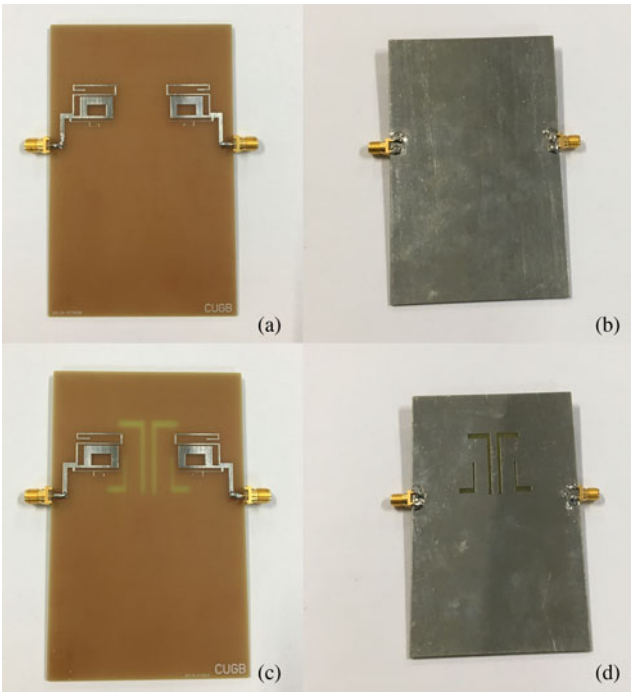

Fig. 3. (a) Top view of the original antenna, (b) bottom view of the original antenna, (c) top view of the decoupled antenna, (d) bottom view of the decoupled antenna.

MIMO antenna. The proposed MIMO antenna system with decoupling elements was simulated and optimized using CST Microwave Studio.

Simulated and measured results

In this part, we will discuss the simulated and measured results. To validate the simulation, a prototype of the proposed multiband MIMO antenna was fabricated according to the optimized dimensions. It was measured using vector network analyzer (Rohde & Schwarz ZNB8). In the experimental measurement, the proposed MIMO antenna is fabricated on a printed circuit board. The test diagram is shown in Fig. 2. The photograph of the fabricated antenna prototype is shown in Fig. 3. Figures 3(a) and 3(b) show the top and the bottom of the original antenna. Figures 3(c) and 3(d) give the top and the bottom views of the decoupled antenna.

S-parameters

The simulated and measured *S*-parameters of the proposed MIMO antenna configuration are shown in Fig. 4. As can be seen from Fig. 4, these results are in good consistency. It indicates that the simulated model is reasonable. There are some deviations between the measured results and the simulated results, which may be due to the difference between the simulation accuracy and the actual test, as well as the interference of noise in the non-anechoic chamber test environment. Since the structure of the antenna is relatively symmetrical, $|S_{11}| = |S_{22}|$, we only give the curve of $|S_{11}|$. In addition, according to the principle of reciprocity antenna, $|S_{21}| = |S_{12}|$, it only shows $|S_{21}|$ in Fig. 4. Since the effect of the decoupling structure on the return loss S_{11} of the antenna is not significant, only the simulated and measured results of the decoupling antenna $|S_{11}|$ in dB are shown in Fig. 4(a). The

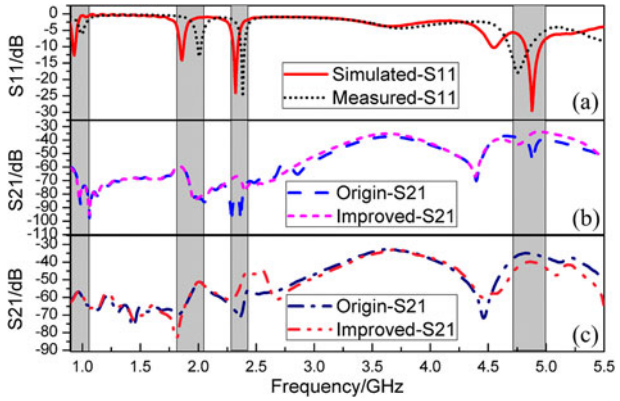

Fig. 4. (a) Simulated and measured S_{11} of antenna, (b) simulated S_{21} of antenna with/without decoupling elements, (c) measured S_{21} of antenna with/without decoupling elements.

Table 2. The operation bands and frequency range of the proposed antenna

Wireless applications	Frequency band (GHz)	Center frequency (GHz)
GSM900	0.88–0.96	0.93
PCS	1.89–1.99	1.86
LTE2300	2.3–2.4	2.322
5G	4.8–5	4.878

operation bands and the frequency range of the proposed antenna are listed in Table 2.

It can be also seen from Fig. 4 that the designed antenna has a better *S*-parameter at the corresponding frequency band and return loss $|S_{11}|$ can basically reach below −10 dB. Since the loss of the dielectric board FR4 is large, the $|S_{21}|$ of the antenna is lower. Due to machining errors, test instrument accuracy and other reasons, the measured results are slightly different from the simulated results, but are still within the coverage of the frequency band. The return loss $|S_{11}|$ can also reach below −10 dB. It can be noted from Figs 4(b) and 4(c) that after increasing the decoupling element, coupling level $|S_{21}|$ dropped significantly at 5G frequency band. Moreover, the isolation of the measured results can be increased at least 5 dB.

Radiation patterns

In order to have a further study of the proposed MIMO antenna with decoupling elements, its performance is discussed in this part. Since the antenna is located in the *x*-*y* plane, the radiation energy of the MIMO antenna is mainly focused in the +*z* direction. To further confirm this point, Fig. 5 shows the 2D radiation pattern of the *E*-plane (*x*-*z* plane) and Fig. 6 shows the 2D radiation pattern of the *H*-plane (*y*-*z* plane) at four operating frequency, respectively. Because the decoupling element has no effect on the radiation, the radiation pattern before and after the improvement does not change much. Hence, the radiation pattern of the original antenna is not shown. Figures 5(a)–5(d) show simulated radiation patterns of modified MIMO antennas on the *E*-plane at 0.93, 1.86, 2.32, and 4.87 GHz, respectively. Figure 6 shows the simulated radiation pattern of the improved

https://doi.org/10.1017/S1759078719000096 Published online by Cambridge University Press

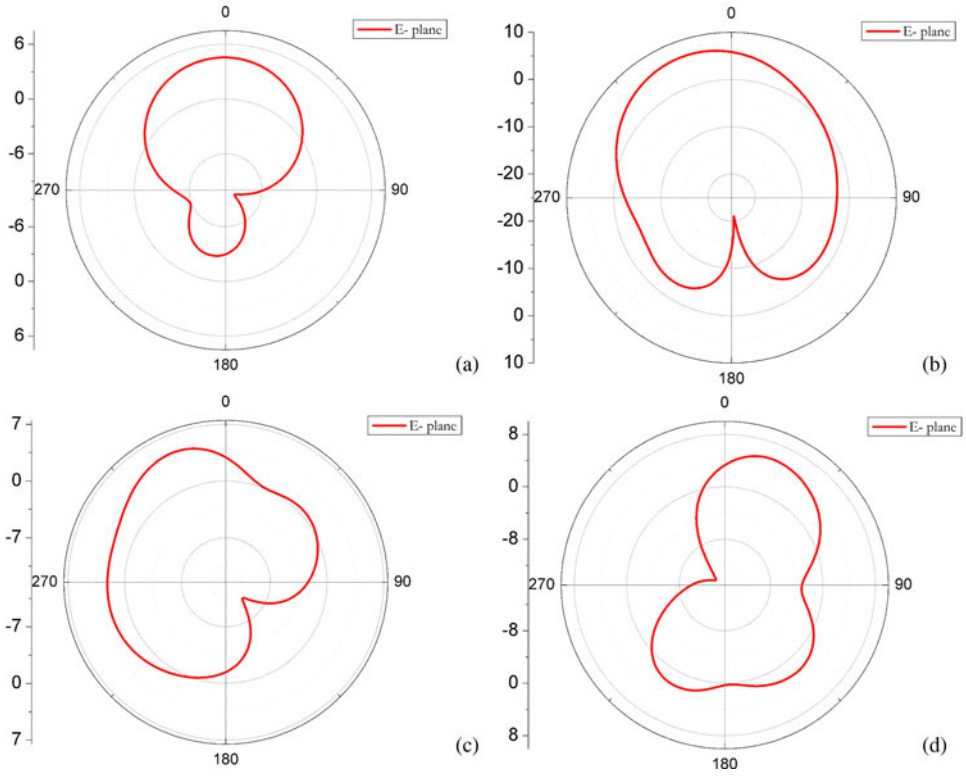

Fig. 5. (a) *E*-plane at 0.93 GHz, (b) *E*-plane at 1.86 GHz, (c) *E*-plane at 2.32 GHz, (d) *E*-plane at 4.87 GHz.

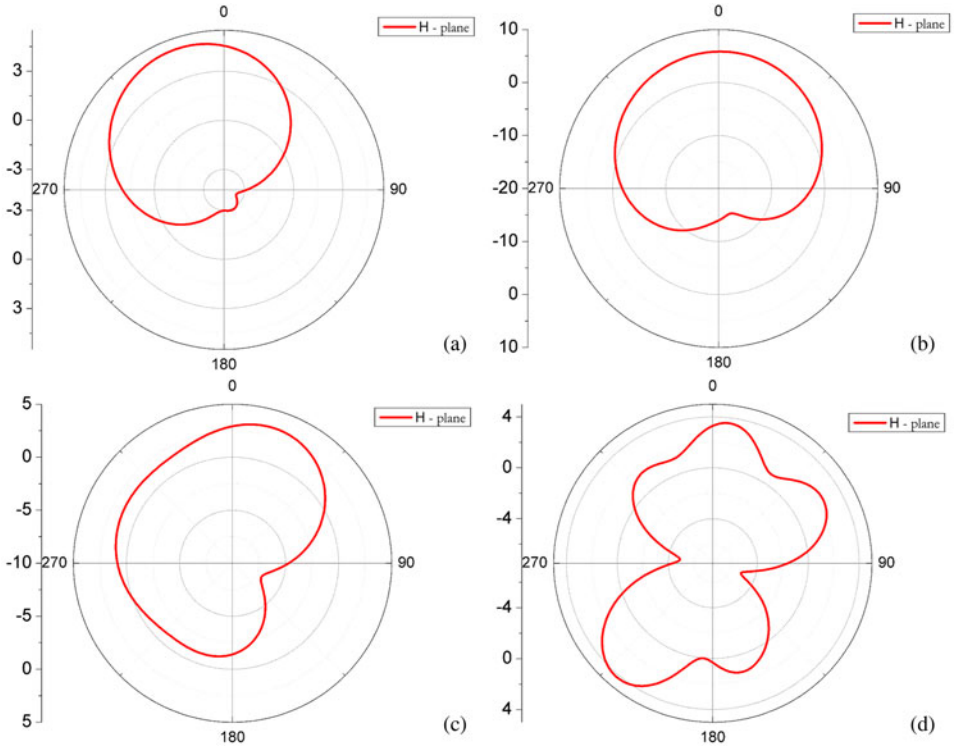

Fig. 6. (a) *H*-plane at 0.93 GHz, (b) *H*-plane at 1.86 GHz, (c) *H*-plane at 2.32 GHz, (d) *H*-plane at 4.87 GHz.

MIMO antenna with four resonance points at the *H*-plane. From Fig. 5, it can be noticed that the proposed antenna has a strong radiation energy in the *z*-direction. These results are consistent with our judgment.

The simulated peak gain values of original antenna are 4.864 dBi at 0.93 GHz, 6.587 dBi at 1.83 GHz, 5.803 dBi at 2.322 GHz, and 7.254 dBi at 4.878 GHz, respectively. Correspondingly, the radiation gain values of decoupling antenna are 4.829, 6.605, 5.385, and

https://doi.org/10.1017/S1759078719000096 Published online by Cambridge University Press

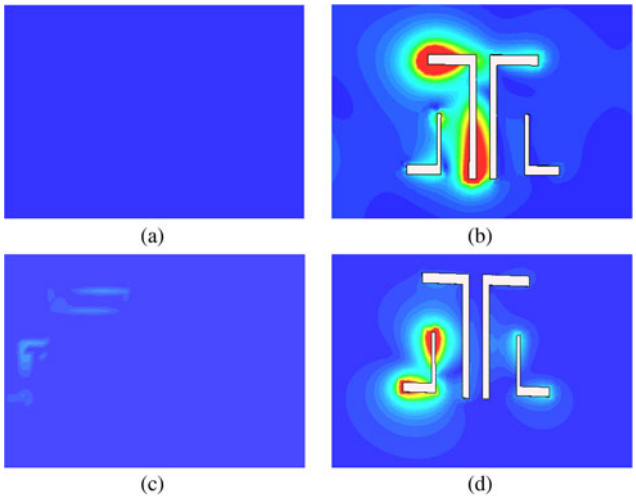

Fig. 7. (a) Surface current distribution without decoupling elements at 2.32 GHz, (b) surface current distribution with decoupling elements at 2.32 GHz, (c) surface current distribution without decoupling elements at 4.87 GHz, (d) surface current distribution with decoupling elements at 4.87 GHz.

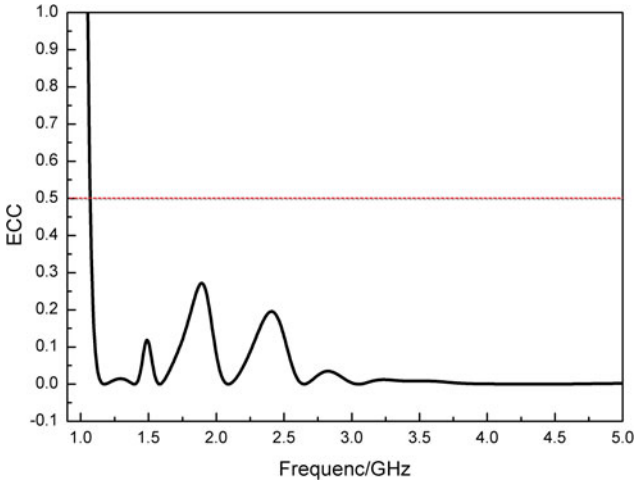

Fig. 8. ECC of decoupling antenna.

Table 3. The comparison of proposed antenna and similar published works

	Geometrical dimensions (mm^3)	Type of substrate	Number of bands	Decoupling mechanism	Whether include 5G
Proposed antenna	76 × 120 × 1	FR4	4	Slotted ground plate to change current path for energy consumption	Yes
[4]	61 × 65 × 0.8	RO4350B	2	A defected ground structure (DGS) with two resonances	No
[8]	50 × 130 × 1.6	FR4	1	Using meander branch shape between two antenna elements	No
[11]	50 × 70 × 0.8	FR4	1	Using decoupling network embedded between dual antennas	No

5.539 dBi. Based on the above comparison, it can be known that increasing the decoupling structure does not change the performance of the antenna such as the operating frequency band, radiation pattern, and gain. So it does not affect the performance of the antenna. Therefore, the decoupling structure can achieve a reduction in electromagnetic coupling between two antenna elements without changing the antenna size.

Surface current

In this paper, in order to reduce the mutual coupling between the two antenna elements, a decoupling structure is etched on the ground plane, which consists of four inverted-*L* branches. Further analysis of the working mechanism of the decoupling element has been studied here. The effect of the decoupling element on the MIMO antenna is analyzed through simulation, as shown in Fig. 7. By slotting the ground plate, the path of the current is changed to a certain extent, so that energy is consumed and the degree of coupling is reduced. Figures 7(a) and 7(b) show the simulated surface current distribution on the MIMO antenna with and without the decoupling structure at 2.32 and 4.87 GHz, respectively. As it can be seen from Figs 7(a) and 7(b), when the frequency is 2.32 GHz, the radiation on the lager inverted-*L* branch is very strong. It is not difficult to be seen from Figs 7(c) and 7(d) that there is a strong resonance at the smaller inverted-*L* structure at 4.87 GHz. Energy is consumed by slotting on the ground plane and the effect of the decoupling is achieved. In order to reduce isolation, to achieve better low coupling, the size of inverted-*L* groove is optimized, such as length and width, and the position of the inverted-*L* groove. The experimental and simulation data demonstrate that the proposed decoupled structure can be applied to the MIMO antenna ideally.

Envelope correlation coefficient

In addition to return loss, the envelope correlation coefficient (ECC) is also a key parameter for evaluating MIMO antenna's performance. ECC indicates the diversity performance of the MIMO antenna. This is an important indicator of whether an antenna can be used in a MIMO system. It can mainly be based on the antenna *S*-parameters calculation formula (1) [17]. For good diversity, ECC should be <0.5. The ECC calculated from the simulated *S*-parameters is shown in Fig. 8. It can be clearly seen from the figure that after the decoupling structure is increased, other resonance points have reached the technical requirements of <0.5 except at 0.93 GHz. Especially at 4.87 GH, it is already close to zero. It proves that the antenna has good

https://doi.org/10.1017/S1759078719000096 Published online by Cambridge University Press

diversity performance. Meet the design requirements. This result is enough to prove that it has very good diversity.

$$\rho = \frac{|S_{11}^{*}S_{12} + S_{21}^{*}S_{22}|^2}{(1-(|S_{11}|^2+|S_{21}|^2))(1-(|S_{22}|^2+|S_{12}|^2))}. \quad (1)$$

In addition, in order to distinguish our results from other existing works, geometrical dimensions, type of substrate, number of bands, decoupling mechanism, and other properties are compared in Table 3. It can be observed that the proposed MIMO antenna has more operating bands, including present 5G bands. It is more suitable for 5G smartphones.

Conclusion

This paper mainly studies a multi-frequency MIMO antenna system including GSM900, PCS, LTE2300, and 5G bands. The proposed MIMO antenna system consists of two symmetrical printed monopole antennas and a decoupling structure. The corresponding radiation branch is added so as to achieve the coverage of 5G frequency band. This is a highlight of this paper. Simulation and experimentation have confirmed that the performance of MIMO antenna system is desired. By adding the decoupling elements, the antenna in the LTE2300 and 5G bands at the isolation effect has been enhanced. Compared with other decoupling methods, the proposed new decoupling element not only has a simple structure but also provides a good decoupling level for closely spaced antennas. Due to the compact size, the proposed decoupling element is a suitable solution for miniaturization.

Acknowledgement. Ziyu Xu and Linyan Guo thank Xinwei Fan and the Open Lab of Rohde & Schwarz (China) Technology Co., Ltd. for the testing support. This work was supported by the National Natural Science Foundation of China (NO. 41704176, 41574131), the National Key Research and Development Program of China (NO. 2017YFF 0105704), and the Fundamental Research Funds for the Central Universities from China.

References

1 **Gunduz D, Khojastepour MA, Goldsmith A and Poor HV** (2010) Multi-hop MIMO relay networks: diversity-multiplexing trade-off analysis. *IEEE Transactions on Wireless Communications* **9**, 1738–1747.
2 **Xu Z, Sfar S and Blum RS** (2010) Receive antenna selection for closely-spaced antennas with mutual coupling. *IEEE Transactions on Wireless Communications* **9**, 652–661.
3 **Lu S, Hui HT and Bialkowski M** (2008) Optimizing MIMO channel capacities under the influence of antenna mutual coupling. *IEEE Antennas & Wireless Propagation Letters* **7**, 287–290.
4 **Cheung SW, Li QL, Wu D, Zhou CF and Wang B** (2017) Defected ground structure with two resonances for decoupling of dual-band MIMO antenna. IEEE International Symposium on Antennas and Propagation & Usnc/ursi National Radio Science Meeting IEEE, 1645–1646.
5 **Chiu CY, Cheng CH, Murch RD and Rowell CR** (2007) Reduction of mutual coupling between closely-packed antenna elements. *IEEE Transactions on Antennas & Propagation* **55**, 1732–1738.
6 **Rahmat-Samii Y and Mosallaei H** (2002) Electromagnetic band-gap structures: classification, characterization, and applications. Antennas and Propagation, 2001. Eleventh International Conference on IET, 560–564 vol. 2.
7 **Li Q and Feresidis AP** (2011) Miniaturised slit-patch EBG structures for decoupling PIFAs on handheld devices. Antennas and Propagation Conference IEEE, 1–4.
8 **Okuda K, Sato H and Takahashi M** (2016) Decoupling method for two-element MIMO antenna using meander branch shape. 2015 International Symposium on Antennas and Propagation (ISAP), Hobart, TAS, Australia. IEEE.
9 **Sato H, Koyanagi Y, Ogawa K and Takahashi M** (2014) A decoupling method for MIMO antenna arrays using branch shape elements. *Ieice Communications Express* **3**, 330–334.
10 **Gil I and Fernández-García R** (2016) Study of metamaterial resonators for decoupling of a MIMO-PIFA system. International Symposium on Electromagnetic Compatibility – Emc Europe IEEE, 52–556.
11 **Zhang XY, Xue CD, Cao YF and Ding CF** (2017) Compact MIMO antenna with embedded decoupling network. IEEE International Conference on Computational Electromagnetics IEEE, 64–66.
12 **Wu D, Cheung SW, Li QL and Yuk TI** (2016) Decoupling using diamond-shaped patterned ground resonator for small MIMO antennas. *Iet Microwaves Antennas & Propagation* **11**, 177–183.
13 **Li JF, Chu QX and Huang TG** (2012) A compact wideband MIMO antenna with two novel bent slits. *IEEE Transactions on Antennas & Propagation* **60**, 482–489.
14 **Toktas A** (2017) G-shaped band-notched ultra-wideband MIMO antenna system for mobile terminals. *Iet Microwaves Antennas & Propagation* **11**, 718–725.
15 **Wang Y and Du Z** (2014) A wideband printed dual-antenna with three neutralization lines for mobile terminals. *IEEE Transactions on Antennas & Propagation* **62**, 1495–1500.
16 **Xu S, Zhang M, Shi X, Liu D, Wen H and Wang J** (2017) Anisotropic metamaterial based decoupling strategy for MIMO antenna in mobile handsets. International Workshop on Antenna Technology: Small Antennas, Innovative Structures, and Applications IEEE, 34–37.
17 **Blanch S Romeu J and Corbella I** (2015) Exact representation of antenna system diversity performance from input parameter description. *Frequenz* **39**, 705–707.

Ziyu Xu was born in Hebei Province, China in 1994. She received her B.E degree in Measurement and Control Technology and Instrumentation from China University of Geosciences Beijing in 2017. Currently she is a master student of University of Geosciences, Beijing. Her main research interest includes the MIMO antenna, decoupling.

Qisheng Zhang was born in Anhui province, China, in 1978. He received the M.S. degree and the Ph.D. degree, in 2012 from the Geosciences University of China, Beijing, China. He has been working in School of Geophysics and Information Technology, China University of Geosciences, Beijing, China since 2005. He is currently an associate professor in the School of Geophysics and Information Technology. His research interests include system-on-a-programmable-chip technology, measurement technology and instrument, high precision data-converters and geophysical instruments

Linyan Guo was born in Yangcheng City, Shanxi Province, China in 1989. She received the B.E. degree in Electronic Information Science and Technology, in 2011. She also received the M.E. degree in Electromagnetic Field and Microwave Technology in 2013 and the Ph.D. degree in Radio Physics from Central China Normal University, Wuhan, China in 2016, respectively. Currently she is a lecturer of China University of Geosciences, Beijing. Her main research interest include the theory and application of metamaterials, analysis and synthesis of antennas, and Ground penetrating radar.

https://doi.org/10.1017/S1759078719000096 Published online by Cambridge University Press